Am J Cancer Res 2012;2(1):1-21
www.ajcr.us /ISSN:2156-6976/ajcr0000085

Review Article

Infrared spectroscopy and microscopy in cancer research and diagnosis

Giuseppe Bellisola[1], Claudio Sorio[2]

[1]Department of Pathology and Diagnostics, Unit of Immunology, Azienda Ospedaliera Universitaria Integrata Verona, Verona, Italy; [2]Department of Pathology and Diagnostics, General Pathology Section, University of Verona, Verona, Italy

Received August 25, 2011; accepted September 10, 2011; Epub November 22, 2011; Published January 1, 2012

Abstract: Since the middle of 20th century infrared (IR) spectroscopy coupled to microscopy (IR microspectroscopy) has been recognized as a non destructive, label free, highly sensitive and specific analytical method with many potential useful applications in different fields of biomedical research and in particular cancer research and diagnosis. Although many technological improvements have been made to facilitate biomedical applications of this powerful analytical technique, it has not yet properly come into the scientific background of many potential end users. Therefore, to achieve those fundamental objectives an interdisciplinary approach is needed with basic scientists, spectroscopists, biologists and clinicians who must effectively communicate and understand each other's requirements and challenges. In this review we aim at illustrating some principles of Fourier transform (FT) Infrared (IR) vibrational spectroscopy and microscopy (microFT-IR) as a useful method to interrogate molecules in specimen by mid-IR radiation. Penetrating into basics of molecular vibrations might help us to understand whether, when and how complementary information obtained by microFT-IR could become useful in our research and/or diagnostic activities. MicroFT-IR techniques allowing to acquire information about the molecular composition and structure of a sample within a micrometric scale in a matter of seconds will be illustrated as well as some limitations will be discussed. How biochemical, structural, and dynamical information about the systems can be obtained by bench top microFT-IR instrumentation will be also presented together with some methods to treat and interpret IR spectral data and applicative examples. The mid-IR absorbance spectrum is one of the most information-rich and concise way to represent the whole "... omics" of a cell and, as such, fits all the characteristics for the development of a clinically useful biomarker.

Keywords: Molecular vibrations, vibrational spectroscopy, infrared radiation, synchrotron radiation, infrared microspectroscopy, mid-infrared absorbance spectroscopy, cancer biomarker, cancer diagnosis, pre-clinical drug screening, unsupervised multivariate analysis

1. Introduction

Cancer is a multi-step process resulting from the accumulation of irreversible and transmittable genetic aberrations together with the concurrent presence of epigenetic alterations in susceptible cells [1, 2]. These contain thousands of mutations [3], show altered responsiveness to the microenvironment [4], may evade host immune responses [5], select and expand particular cancer cell phenotypes that metastasize and/or become resistant to chemotherapy [6]. Roughly 13.3 million new cancer cases and 7.9 million cancer deaths have occurred worldwide in 2010, respectively. Because of population ageing, these numbers are projected to rise to 15,0 million new cases and 9.0 million deaths in 2015 and 21.4 million new cases and 13.1 million deaths in 2030, respectively [7]. However, at least ~30% of all cancer cases and roughly ~40% of all cancer deaths should be potentially avoidable through primary prevention of common modifiable risk factors [8, 9] and by improving early detection and treatment of amenable cancers when there is still some chance of successful benefit [10]. The development of reliable and affordable technologies for the screening of individuals with cancer, or who are likely to develop it in the future, as well as for improving the early diagnosis of cancer and the prediction of treatment outcomes with the aim of maximizing cure and

reducing morbidity to the lowest possible level may be as important as prevention activities to reduce the incidence of cancer. Therefore, one of the main issues in cancer research is represented by the discovery and validation of new cancer biomarkers.

A biomarker of cancer is any structural and/or functional entity that can be objectively measured such as genes, proteins, metabolites, activities and intermediate pathways, morphologic, cytogenetic and cytokinetic parameters, as well as any specific physical trait or detectable change connected with a cancer disease in human individuals [11]. Different individual analytical methods assembled in multiplexed genomic [12], proteomic [13, 14], and/or cell line-based platforms [15] have been developed and utilized for the discovery of new cancer biomarkers. These platforms are often associated also with high resolution imaging tools such as different microscope techniques [16]. The generation of an ever-increasing amount of high-throughput of data implies the analysis of large data sets by sophisticated algorithms and bioinformatics tools. These are utilized to identify individual markers of interest or to derive signatures and/or patterns of many markers. Therefore, analytical platforms are generally integrated within computational biology and bioinformatics facilities that are necessary to analyze, associate and correlate large amounts of data obtained from different sources [17, 18]. Technologies and biomarkers must be tested and validated in pre-clinical cell and animal models before undergoing final evaluation and validation in clinical trials and definitively used in clinics [19, 20]. These steps are necessary to define the performances of each test (e.g. analytical variability, sensitivity, specificity, reproducibility, and reliability of the measurements) and to obtain experimental evidence on the accuracy levels with respect to the suggested application (screening, diagnosis, prognosis, therapy follow up). The results of this multidisciplinary approach ultimately need to meet with the acceptance of final users, mainly oncologists and pathologists who will perform clinical trials.

The evaluation and validation of a cancer target biomarker implies costly and lengthy processes, especially for tests that are proposed for cancer screening. An ideal test requires poor sample manipulation and it has to be possibly non-invasive, highly sensitive, specific and reliable as well as affordable to reduce the costs of clinical trials. Unfortunately, these characteristics do not properly fit different "…omics" platforms that still are too expensive, and/or scarcely reliable for screening applications. Hence a high demand for developing new and complementary easily available analytical methods.

Advances in biophotonics – a combination of biology and photonics concerning with the generation, emission, transmission, modulation, signal processing, switching, amplification, detection and sensing of light – have broken the resolution (lateral resolution) of conventional light microscopes. Resolutions at length scales of tens to hundreds of nanometers have been achieved, mostly in combination with fluorescence probes, allowing the localization of single molecules with nanometer precision and the imaging of many cellular processes taking place within these diffraction-limited distances [21]. It is expected that the applications of these technologies for imaging will be enable researcher in the elucidation of the dynamics of cell components interactions within cancer cells allowing significant advances in understanding cancer pathophysiology as well as to influence cancer biomarker and anticancer drug discovery. The parallel improvements of technologies for high resolution imaging of cancer in vivo [22, 23] might facilitate the detection and/or imaging of the smallest possible number of cancer cells in solid tumours, ideally before the "angiogenic switch" [24]. Moreover, also the use of nanotechnology may help in achieving this goal [25] since most current techniques for in vivo molecular imaging still detect cancer at a stage in which the disease is too far advanced to be cured [26].

Since the middle of 20th century infrared (IR) spectroscopy coupled to microscopy (IR microspectroscopy) has been recognized as a non destructive, label free, and highly sensitive and specific analytical method with many potential useful applications in different fields of biomedical research and in particular cancer research [27-29]. Fourier transform (FT) infrared (IR) spectrometers were commercially introduced in 1970. They were characterized by peculiar analytical performances that mainly consisted in the use of trace sample (down to 100 ng), high throughput measurements without sample destruction and with minimal sample preparation,

frequency precision and reproducibility, rapid-scan analysis, and computerized data handling and storage. Their principal limitation was (and still is) the low spatial resolution at the focus point in the sample resulting in a measured sample area in the order of square millimeters. After various events, only in the 80's the first commercial infrared microscope designed exclusively for FT-IR spectrometers became available allowing to perform FT-IR microspectroscopy (microFT-IR). In the past three decades, many other technological improvements have been made to facilitate biomedical applications of microFT-IR extensively reviewed in [30] which has been successfully applied to samples from a variety of cell lines [31], blood cells [32, 33], and tissues [34] included cervix [35], breast [36, 37], prostate [38], lung [39], colon [40, 41], brain [42-44], skin [45-47], esophagus [48], liver [49], lymph system [50, 51] and stem cells [52-56]. The results of all those studies have clearly indicated that microFT-IR associated with the use of some appropriate statistical data analysis methods [57] has an accuracy in classifying normal and malignant tissues/cells in the order of 80-100%. In spite of its many advantages, the application of microFT-IR to cancer research and clinical diagnostics continues to be 'under strong development' or 'promising' and to the best of our knowledge, no microFT-IR system has been put in clinical trials for cancer screening or diagnosis to date. On the contrary, it is long since applied in microbiology where it allows the rapid and inexpensive characterization and classification of microorganisms [58, 59]. This underuse of microFT-IR has been mainly ascribed to the difficulty of directly applying this technique in vivo, to its relatively low spatial resolution mostly confined to the micrometric scale as well as to a certain complexity in treating and interpreting data, a feature, however, that is shared with other analytical applications. Although recent technological improvements [60] may represent new reasons for hope to introduce microFT-IR spectroscopy and imaging into clinics [61] one can also suspect that this powerful analytical technique has not yet properly come into the scientific background of many potential end users [62] and de facto it is mainly utilized for research scopes into Synchrotron Radiation (SR) infrared beamlines facilities. This poses the urgent demand also for a more appropriate and generalized interdisciplinary scientific education as well as for more criticism that appears to be necessary for the selection, identification and correct application of appropriate analytical methods in cancer research as well as in the diagnosis and follow-up of cancer diseases.

This review is aimed at illustrating some principles of Fourier transform (FT) IR spectroscopy and microscopy (microFT-IR) to interrogate molecules in specimen by mid-IR radiation. It is not necessary to be a composer to enjoy vibrations from a nocturne of Chopin. Likewise, it is not mandatory to be a physicist to be aware of phenomena that govern interactions between mid-IR radiation and matter. On the contrary, penetrating into basics of molecular vibrations might help us to understand whether, when and how complementary information obtained by IR vibrational spectroscopy and microscopy is useful in our research and/or diagnostic activities. The implications of coupling FT-IR spectrometry with an IR microscope to perform microFT-IR, to obtain spatially resolved chemical images of an object, and to resolve the molecular structure and composition of a sample within a micrometric scale in a matter of seconds will be also presented as well as some limitations of microFT-IR will be illustrated. Some examples of how biochemical, structural, and dynamical information about the systems can be obtained by bench top microFT-IR instrumentation also when no fluorescent probe and/or specific biomarker is available will be also illustrated together with the principal techniques to obtain mid-IR spectra and methods to treat and interpret IR spectral data. The FT-IR absorbance spectrum is one of the most information-rich and concise way to represent the whole "…omics" of a cell and, as such, fits all the characteristics for the development of a clinically useful biomarker.

2. IR radiation and molecular vibrations

Electromagnetic waves existing within a wide, continuous range of frequencies known as the electromagnetic spectrum have been extensively used in cancer research and diagnosis. For instance, the highest energy photons associated with the shortest wavelength, λ, and with the highest frequency, ν, characterize X-rays and Gamma-rays. Opposite, the lowest energy photons, the longest wavelength, λ, and the lowest frequency, ν, characterize the region of radio waves that around 40-50 MHz are used in nuclear magnetic resonance (NMR) and magnetic resonance imaging (MRI). Infrared (IR) radiation spans an interval of electromagnetic spectrum between the red end of the visible

region (λ ~780 nm, ν ~0.38x10^{15} Hz, and $h\nu$ ~1.59 eV) and the beginning of microwaves region (λ = 1 mm, ν = 3x10^{11} Hz, and $h\nu$ = 1.24x10^{-3} eV). Within this IR interval three regions of increasing wavelengths have been recognized: near-IR (λ from ~780 nm to 2.5 μm), mid-IR (λ from 2.5 μm 25 μm), and far-IR (λ from 25 μm to 1000 μm), respectively. The more convenient and the most commonly used spectroscopic unit in the IR region is the reciprocal of the wavelength, 1/λ, called wavenumber, $\tilde{\nu}$, (the number of waves per unit length) with unit of reciprocal centimeter (cm^{-1}). Wavenumber, $\tilde{\nu}$, wavelength, λ, and frequency, ν, are related by the equations **Eq. 1** and **Eq. 2**:

$$\lambda = \frac{c}{\nu} = \frac{1}{\tilde{\nu}} \qquad \text{Eq. 1}$$

$$\tilde{\nu}_{(cm^{-1})} = 10^4 \times 1/\lambda_{(\mu m)} \qquad \text{Eq. 2}$$

Therefore, the IR region of the electromagnetic spectrum has dimension of wavenumbers extending from ~13000 cm^{-1} to ~10 cm^{-1}, with near-IR, mid-IR, and far-IR regions spanning from ~13000 cm^{-1} to 4000 cm^{-1}, from 4000 cm^{-1} to 400 cm^{-1}, and from 400 cm^{-1} to 10 cm^{-1} wavenumbers, respectively.

The range of energy photons in the mid-IR region extends between 0.05 eV and 0.5 eV. Since these energy values fit the quantized vibrational transitions of intra- and intermolecular bonds of bonded atoms in molecules, mid-IR photons can be absorbed by molecules that are in periodic (sinusoidal) motion (molecular vibrations). The frequency of vibration, ν, is related by the Hooke's law to a force constant, f=-$k\Delta_r$, which is proportional to the entity of displacement between the two atoms, Δ_r, and to the reduced mass, m_r=m_1m_2/(m_1+m_2) as illustrated in **Figure 1a**. The frequency, ν, rises when the force constant, f, increases, that is when the electron density in the bond between the two atoms increases, as exemplified in the table of **Figure 1b**. On the contrary, frequency decreases with the increasing values of reduced mass, m_r. The frequency of a vibration, ν, is inversely proportional to the atomic masses and directly proportional to the bond strength and therefore the vibrational mode of a chemical bond and/or a chemical group may occur at a specific frequency.

IR absorbance vibrational spectroscopy

When a sample matter, for instance a pure molecule, is placed in the path of an IR beam light between the source and the detector, the molecule will absorb only the frequency of mid-IR that coincides with the frequency of the vibration allowing the molecule enters in a resonant vibration status. IR absorbance spectroscopy extensively treated in [63-65] measures the loss of IR radiation transmitted through a sample across an interval of frequencies of electromagnetic spectrum. Depending on the selected interval of wavelengths, near-IR spectroscopy, mid-IR spectroscopy, and far-IR spectroscopy (THz spectroscopy) can be performed using near-IR radiation, mid-IR radiation, and far-IR radiation, respectively. Mid-IR absorbance spectroscopy plots the recorded intensity of absorption bands versus an interval of wavenumbers, $\tilde{\nu}$, from 4000 to 400 cm^{-1}, which corresponds to changes of vibrational energy levels from the ground level to the first energy level ($E_0 \rightarrow E_1$) in molecules.

Fundamental vibrational modes (also called normal modes) that are detectable by mid-IR spectroscopy are mainly represented by bond stretching (either symmetric, ν_s, and antisymmetric, ν_{as}) and bond deformations (mainly symmetric and antisymmetric bending, δ_s and, δ_{as} respectively; other vibrational modes are twisting, γ_t, wagging, γ_w, rocking, γ_r, and scissoring motions. Fundamental vibrations concerning with water molecule are shown in **Figure 1c**. In a free H–O–H molecule the antisymmetric and symmetric stretching vibrations (ν_{as} and ν_s, respectively) and the bending (δ) deformations of O–H group occur at ~3500 cm^{-1}, ~1650 cm^{-1}, and ~600 cm^{-1}, respectively. Since the frequency of a vibration is concurrently determined by the bond strength, the vibrational mode and the reduced mass, m_r, of atoms composing chemical groups, the frequencies at which specific vibrations occur within the spectrum are fairly constant for a given functional group (e.g., –CH_2, –C=O, O–H, etc.), as summarized in **Table 1**. For instance, the stretch of methylene group, (ν_{as} CH_2 and ν_s CH_2), in molecules occur between ~2950 cm^{-1} and ~2860 cm^{-1}, respectively. As indicated in the harmonic oscillator model of **Figure 1a**, each of the two atoms (or groups) connected by the bond has an associated charge. If the two atoms are identical (e.g. O_2, N_2, etc.) and only one fundamental vibration

a

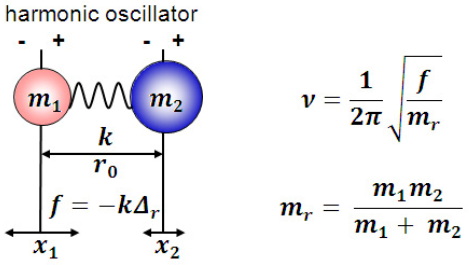

b

group	m_r (amu)*	ν (wnr., cm^{-1})
C–H	0.92	~3000
C–O	6,86	~1150
C–Br	10,44	~600
C–C	6,00	~1100
C=C	6,00	~1650
C≡C	6,00	~2300

amu, atomic mass unit; ν, stretching mode

c

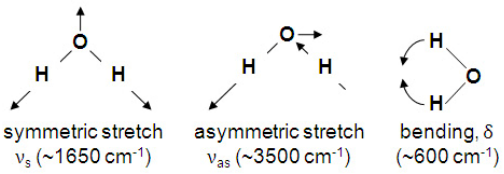

Figure 1. The basis of infrared (IR) vibrational absorbance spectroscopy. **a**. The classical harmonic oscillator model. **b**. Some examples illustratint the relationships among atomic masses, bond strength and a particular vibrational mode (stretching) of some chemical groups. **c**. Fundamental vibrational modes of a molecule of free water detectable at specific frequency values within the mid-IR region of the electromagnetic spectrum.

can occur, e.g. ν_s , there will be no net change of dipole moment during the vibrational transition and therefore there will be no detectable mid-IR activity. Therefore, also net change in the dipole moment must occur in the group molecule in order for a particular vibrational mode to be detectable by mid-IR spectroscopy. For instance, the planar CO_2 molecule has no permanent dipole moment, since the individual bond dipoles exactly cancel each other during symmetric stretching vibration (ν_s O–C–O) occurring at ~1480 cm^{-1}. Nevertheless, the antisymmetric stretching, ν_{as} O–C–O at ~2560 cm^{-1} and the bending vibrations δ O–C–O at ~500 cm^{-1}, respectively can be detected because there is a net change in the dipole moment of CO_2 molecule at those wavenumbers allowing this molecule becomes detectable by mid-IR radiation. Moreover, also the magnitude of the dipole moment change determines the intensity of absorption band. For instance, whereas the νC=O bands have strong absorbance values more symmetric vibrations such as νC=C have weaker absorbance values or even they are not absorbing.

A tri atomic, angular molecule like H_2O produces 3 normal vibration modes: one symmetrical, one asymmetric stretching vibration and a bending vibration (**Figure 1c**). In general, a polyatomic nonlinear molecule with N atoms has 3N–6 distinct vibrations (six results from three translational and three rotational movements of the whole molecule, respectively). In linear molecules such as CO_2, the number of possible vibrations is 3N–5 (4 vibrational modes for CO_2). For human albumin, a protein of 609 amino acids with > 9000 atoms, the number of possible vibrations results > 27000 if we assume an average of 15 atoms per amino acid [66]. Stretching vibrations of O_2 and N_2 as well as of many other non-IR active modes can be detected by Raman spectroscopy. Its principle of functioning is based on the selective inelastic scattering of a photon induced when a monochromatic radiation (any excitation laser wavelength can be used) interacts with molecules that change their polarizability. A small fraction of light is scattered by an excitation associated with vibrational and rotational transitions of the molecule. The associated emerging photons of lower or of higher energy (frequency) can generate Stokes and anti-Stokes lines that in the Raman spectrum become detectable as shifts of frequency (Raman shifts) with respect to the incident radiation. Also this complementary spectroscopic technique, that will be not described longer in this review, has many potential application in cancer research and diagnosis [67-69].

3. IR vibrational spectroscopy and microscopy

All modern IR spectrometers use Fourier transform (FT) and are composed of the following common elements: an internal IR light source, the interferometer (basically a Michelson interferometer), and a single element detector connected with an amplifier and a computer [63]. The internal IR light is generated by a broadband, polychromatic continuum, conventional thermal light source such as a heated silicon

carbide rod (Globar). Destructive or constructive interferences between IR light and matter are generated in the interferometer which consists of a system of mirrors, a stationary mirror and a moving mirror, and a semireflective lens (the beamsplitter, usually made of KBr). These interferences are recorded by the detector as a sinusoidal variation of intensity (cosine function) to the optical retardation which is Fourier transformed (FT) to a spectrum (intensity as function wavenumbers, $\tilde{\nu}$). For a monochromatic radiation this results in a single line (band). With a broadband source (polychromatic, continuum source), constructive and destructive interferences in the spectral domain transmitted to and recorded by the detector will generate an interferogram. This represents the summation of all the cosine functions of all the individual wavelengths present in the source and zero path difference (ZPD) positions where all interferences will be in phase (the centre-burst). The application of mathematical function Fourier transform will convert this interferogram into a mid-IR single-beam spectrum where the number of peaks will reflect the number of detectable components in the sample. The intensity in peaks, reflecting the amount of different molecular bonds absorbing in specific regions of the IR spectrum, will be in relation with the relative abundance of different sample constituents. The minimum wavenumber difference that can be distinguished between two lines in a spectrum corresponds to spectral resolution [64].

FT-IR absorbance spectroscopy without a microscope has absent or very limited spatial resolution [70] and the sample spectrum limits to reflect the average biochemical and structural information referred to the whole probed sample. The addition of an FT-IR microscope to the IR spectrometer has realized the possibility to detect vibrational motions of molecules within very restricted regions of the sample allowing the development of microFT-IR spectroscopy. The schematic layout of a typical microFT-IR apparatus is shown in **Figure 2**. This apparatus is used to associate the optical image of selected object, for instance an individual cell, with the corresponding IR spectrum or its chemical image.

The FT-IR microscope is similar to visible light microscope but it does not employ glass refrac-

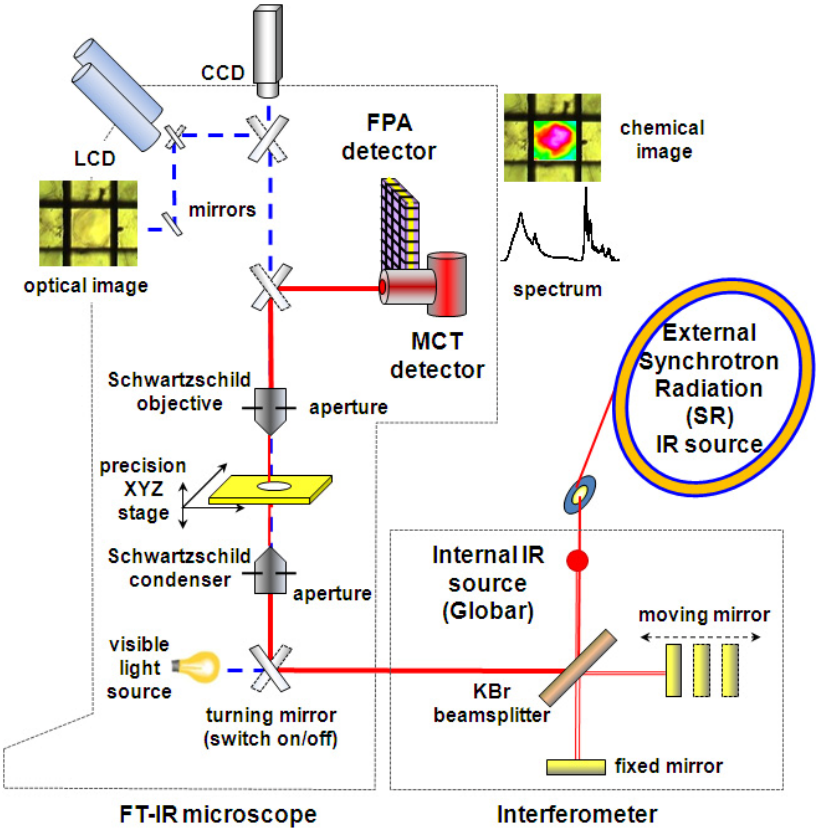

Figure 2. The schematic layout of components in an microFT-IR apparatus. The external IR beam is generally provided by Synchrotron Radiation and a dedicated beamline is required to extract IR light from the storage ring of a Synchrotron and to collimate IR light to the experimental area where the microFT-IR apparatus is usually located several meters from the exit port. The description of microFT-IR apparatus and the functioning of single components are in the text.

tive elements (glass is opaque to IR light of $\lambda >$ ~5μm). For this reason microFT-IR performed in transmission (described in 3.1) requires that probing samples are deposited on optical windows (e.g. ZnSe, CaF_2, and BaF_2 crystals) that do not absorb, or absorb very low mid-IR radiation and have very high values of transmittance within a wide range of frequencies in the mid-IR region. Switching on the separate visible light source and associated optics, the IR microscope works like a standard optical microscope allowing the sample can be inspected by eyepiece. Several spot areas can be selected (and marked) moving the computerized precision XYZ sample stage. Digitalized images can be recorded by a Charged-Coupled Device (CCD) camera in order to associate the image of selected object visualized in the Liquid Crystal Display (LCD) or on the computer screen with its corresponding FT-IR absorbance spectrum.

IR microscopes make use of Schwartzschild objectives (typically a combination of concave and convex mirrors aligned about the optical axis direct the beamlight through a hole) with a numerical aperture (NA) of ~0.61. With the sample placed between the Schwartzschild objective and the condenser, the microscope works in the confocal configuration and generally a spatial resolution of ~$\lambda/2$ is obtained [71]. Adjustable aperture slits of IR opaque material (e.g. glass) allow to delimit selected spot areas from which IR signals will be acquired switching on IR light.

The FT-IR microscope is generally equipped with a single channel highly sensitive mercury cadmium telluride (MCT) photoconductive detector cooled in liquid nitrogen. Through connections with an amplifier the detector transmits the information to the computer. In a typical IR experiment the goal is to obtain reproducible spectra with an acceptable value of signal to noise ratio (S/N) as defined by the ratio of source power (SP) to the noise power (NP). To this scope, enough IR signal must be cumulated on the detector by performing a number of scans in continuous mode within the selected interval of wavenumbers (e.g. from 4000 cm^{-1} to 600 cm^{-1}) at a selected scanner velocity (e.g 40 kHz). Reducing the aperture slits of microscope, the flux of photons to the detector reduces as well as the value of S/N. Increasing the number of scans extends the acquisition time necessary to obtain each spectrum. In order to optimize the acquisition with a single element detector, the number of scans and the aperture sizes must be therefore balanced acting on the SP and/or on the NP terms of the following equation: S/N = SP/NP. Working with a conventional thermal source such as Globar, which emits mid-IR radiation in a 360 degrees distribution, and with aperture sizes reduced to ~20μm x 20μm or less, the photon throughput towards the detector significantly reduces while the detector noise remains constant and the value of S/N is strongly decreased independently on the duration of acquisition. Moreover, working with aperture sizes approaching the wavelength of mid-IR radiation (2.5 μm - 25 μm) the recorded spectra become increasingly distorted due to diffraction effects that give much more difficult the analyses in the spectra and results interpretation. Therefore, to increase S/N values one possibility is to modify the source power, SP, that is to increase the brightness or IR light, for instance using external IR light source from Synchrotron Radiation (SR) [72]. Whereas for aperture values ≥40μm x 40μm there is no substantial advantage of using SR with respect to Globar, the highest brightness of SR IR source provides advantage over Globar for shorter aperture settings (≤20μm x 20μm down to the diffraction limit of ~3μm x 3μm). This is mainly due to the fact that the flux of SR IR photons is not a limiting factor during the acquisition of IR signals. In this situation, spatial resolution becomes diffraction limited [73]. However, when the instrumental setup has been optimized, high quality spectra of individual cells with a diameter of ~15 μm can be obtained also with the conventional and more accessible source Globar, as shown in **Figure 3a**. The two mid-IR absorbance spectra have been obtained from the same individual cell restricted within aperture slits of 15μm x 15μm in sizes and alternatively illuminated with the internal (Globar) and with the external SR IR sources at the B22 IR microspectroscopy end station of Diamond Light Source, respectively. Higher noise, reflecting the lower S/N value, can be observed in the second derivative of the absorbance spectrum obtained with Globar with respect to SR IR spectrum. SR microFT-IR might be therefore considered as a powerful technique to obtain high quality reference spectra or to perform the raster scanning of single cells as illustrated in **Figure 3b**. However, the scope of this simple experiment was to demonstrate that microFT-IR analysis on individual cells can be performed also with a conven-

tional IR source which is more advantageous and reliable for routine applications than SR IR microFT-IR absorbance spectroscopy.

Recently, FT-IR microscopes equipped with a second multichannel Focal Plane Array (FPA) detector have become available [74]. FPA composes of many basic units with a sandwich structure (pixel). Two MCT layers, one detecting photons and the other carrying out signal collection, multiplexing and signal amplification, are respectively fixed together through a soft, electrical conducting material. Each pixel unit, which functions as a discrete MCT detector within the array, allows to record a full IR spectrum within the interval 4000–900 cm^{-1}. For an 64x64 FPA detector (up to 256x256 pixel FPA detectors are currently available) there are 4096 pixel units with a spatial area sampled by each pixel unit of ~1-7x1-7 μm^2, depending on the objective magnification. Although the possibility to perform microFT-IR with FPA and SR IR beamlight has been reported [75] microFT-IR with FPA is typically carried out with bench top instrumentations using the more available conventional internal Globar source in a routine lab. No aperture is set with FPA and the single pixel element defines spatial resolution. As compared to the single-point mapping approach which requires acquisition time in the timescale of hours, FPA detectors have dramatically improved the rate at which chemical information can be collected [76] allowing to generate microFT-IR absorbance spectra and images in the timescale of minutes. Rather the problem working with FPA is the extremely large volumes of data generated and associated with chemical images (in the order of gigabytes of data per hour). Chemical images, or spectral "hypercubes", obtained by FPA consist of pixel coordinates, wavelength, and intensity information. The analyses within such spectral "hypecubes" may reveal information on the tissue architecture allowing for instance to distinguish between normal and tumor vasculature and to help the delimitation of areas in corresponding tissues [42].

MicroFT-IR techniques and samples

With a single channel MCT detector microFT-IR analysis can be performed by one of the three following techniques: transmission, transflection which associates absorption with reflection, and attenuated total reflection (ATR). All three techniques are aimed at obtaining IR spectra of high quality in representative samples.

Transmittance represents the traditional means of measuring the mid-IR spectrum of a sample placed on an IR transparent substrate into the path of the IR beam light between the objective and the condenser of an FT-IR microscope. The intensity of mid-IR radiation passing through the sample, I , and reaching the detector is compared to the intensity of mid-IR radiation reaching the detector in the absence of the sample, I_0 (reference background spectrum). The resulting percentage of radiation transmitted, %T, by the pure sample substance at a given wavenumber, can be expressed as (**Eq. 3**):

$$\%T = \frac{I_{(\tilde{\nu})}}{I_{0(\tilde{\nu})}} \times 100 \qquad \text{Eq. 3}$$

The transmittance, T, of the sample at a particular wavenumber, $\tilde{\nu}$, is given by $I_{(\tilde{\nu})}/I_{0(\tilde{\nu})}$ and has values between 0 and 1. The lower the value of transmittance, T, and the more mid-IR radiation is absorbed through the sample of thickness (pathlength), l (in cm).

The corresponding amount of mid-IR radiation absorbed, A, by the pure sample substance at $\tilde{\nu}$ is expressed as (**Eq.4**):

$$A_{(\tilde{\nu})} = \log_{10}\frac{1}{T_{(\tilde{\nu})}} = \log_{10}\frac{I_{(\tilde{\nu})}}{I_{0(\tilde{\nu})}} \qquad \text{Eq. 4}$$

where A is the absorbance. The Beer's Law expressed by the following equation (**Eq. 5**):

$$A_{(\tilde{\nu})} = a_{(\tilde{\nu})}lc \qquad \text{Eq. 5}$$

Relate the absorptivity of a pure substance, $a_{(\tilde{\nu})}$ at a wavenumber, $\tilde{\nu}$, in the mid-IR to the concentration of the sample, c, and to the relative number of absorbing molecules, lc. Therefore, using a calibration procedure quantitative information on sample components can be obtained by microFT-IR [75].

Information that can be obtained may concern

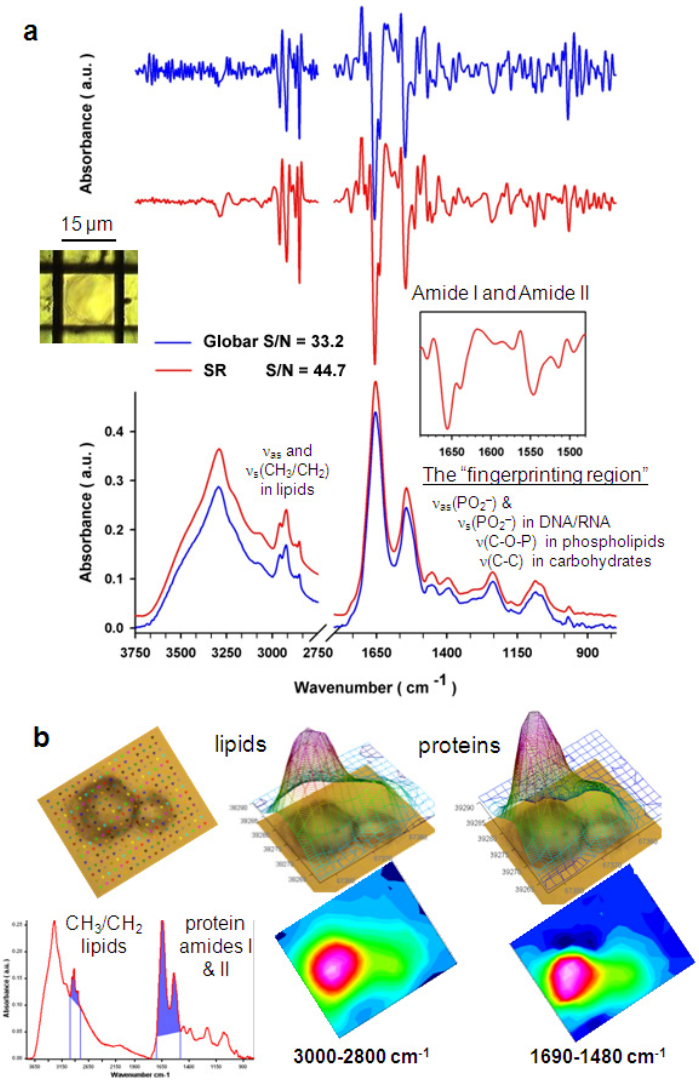

with the variations of a single component, for instance as a consequence of dynamic changes occurring during a biochemical reaction [77] or reflecting the different biochemical composition within samples of different tissues and body fluids or among specimen from different individuals, as well as variations of many spectral components associated, for instance with the presence of oncogenic viruses [78, 79] , different states of cancer aggressiveness [80] and/or the different sensitivity to anticancer drugs [81, 82].

As in any other experimental design, also in microFT-IR analysis sample preparation represents an important aspect to obtain qualitative and quantitative information on samples. However, as compared to other analytical techniques micro-FT-IR does not require extended sample manipulations. The major technical problem is water which strongly absorbs mid-IR light masking vibrational absorption of other important molecules such as proteins, lipids, amino acids, carbohydrates, and other molecules within the sample [83]. Therefore, although <10 µm of bulk water can be acceptable since it can be subtracted in spectra by a

Figure 3. Fourier transform infrared microspectroscopy (microFT-IR) on individual cell. **a**. The FT-IR absorbance spectrum of an individual human formalin-fixed and air-dried monocyte deposited on ZnSe window within the sampling interval of wavenumbers 3750-800 cm^{-1}. The selected cell (36x magnification) was restricted by slits within a 15 µm x 15 µm sample area. This was alternatively illuminated with IR light from a broadband internal source (Globar, blue trace) and with beam of IR light from Synchrotron Radiation (SR, red trace) focused on the sample, respectively. To obtain acceptable signal to noise ratio (S/N) values a number of 128 scans was cumulated (velocity 20 kHz, spectral resolution 4 cm^{-1}, total acquisition time 60 s) on a nitrogen cooled single element MCT detector with a detecting area of 50 x 50 $µm^2$. The background (ZnSe) spectrum was collected from a 15 µm x 15 µm area external to the sample. Atmosphere water vapour and CO_2 were compensated and the baseline was corrected using appropriate algorithms in the software. The superimposed second derivative spectra have been calculated by a generalized Savitzky-Golay smoothing algorithm on 9 points. The contribution of sub-bands in the markers peaks of amide I and amide II within the interval 1690-1480 cm^{-1} of SR IR spectrum has been highlighted in the framed box. **b**. The mapping of an individual formalin-fixed and air-dried cell by SR microFT-IR. The selected area was raster-scanned by collecting a series of spectra from 18x15 points grid (10 µm x 10 µm area, 2 µm step, 256 scans within the interval 4000-600 cm^{-1}, scanner velocity 20 kHz, spectral sensitivity 8 cm^{-1}, one background area every five sample spectra) on a single channel 100 µm x 100 µm MCT detector. The spectra were assembled and integrals were calculated within the interval of wavenumbers between 3000 and 2800 cm^{-1} (symmetric and antisymmetric stretching of CH_3 and CH_2 groups in lipid molecules) and between 1690 and 1480 cm^{-1} (amide I and amide II modes in proteins), allowing to obtain the two dimensional distribution of lipid and proteins, respectively. The intensity scale of false colors extends from the lowest absorbance (blue) to the highest absorbance (red-violet) values in the two dimensional contour maps superimposed to the underlying object, respectively.

software algorithm, microFT-IR is preferentially carried out on dried samples. The rapid dehydration or formalin fixation can be performed to remove water from hydrated cells and tissues with no or minimal effects on the mid-IR spectrum [84]. Cells from cell cultures can be deposited by the simple drop method or can be spun on the appropriate substrates where they are air -dried. It is worth of note that the mid-IR spectra of hydrated cells grown in adherence on biocompatible and IR transparent substrates have been already described [85-87] and that the development of appropriate microfluidic devices might allow to investigate dynamical processes also in living cells [83, 88].

Sample thickness, the material dispersion on the substrate (cells, portions of cells) and the intrinsic homogeneity of biochemical components within cells and tissue samples can influence the absorption spectra [89]. Since the measured absorbance, A, follows the Beer's Law, samples thickness, l, might be between 3 and 10μm in order to obtain intensities of absorbance in peaks that are distinguishable from the background noise in very thin samples as well as to avoid the saturation of some bands in thicker samples. An ideal sample has a flat surface with a constant sample thickness within the probing area so that the non absorbed IR light that emerges from the sample and reaches the detector results parallel to the incident light. However, by some computational approach different thickness within sample and among samples (different optical pathlengths, l) can be minimized to compare the intensity of absorbance in marker peaks.

MicroFT-IR with single detector should be preferentially performed selecting several probing areas (e.g. 50μm x 50μm with 36 x magnification) on the most homogeneous zones of the sample. Also an individual cell is a heterogeneous object which can changes its shape and composition, for instance during its differentiation [90-92], within the phases of cell cycle [93, 94], as a consequence of changes in the culture medium [95] or during the induction of cell death by physical, chemical or drug agents [51, 96-102]. Curiously, relatively large, dense patches of chromatin can block IR light from passing in some locations allowing unexpected reduced absorbance of DNA as an artifact in the spectrum of cells [103]. Moreover, IR light passing through cells can be deviated from its original path and this scattering effect becomes evident in the mid-IR spectra of single cells presenting broad oscillating baselines, shifted peak positions and distorted peak shapes [104]. This scattering effect has been attributed to significant losses of mid-IR light with wavelengths fitting the sizes of a cell and/or of its intracellular components. For instance, the nucleus may result in resonant scattering (Mie scattering) [105]. Distortions due to resonant Mie scattering can be corrected using an appropriate algorithm [106].

Transflectance (**Figure 4**) couples absorption and reflection through the sample [107]. It realizes when cells and tissues are lied on a glass slide coated with a thin layer of silver (low-e microscope slide) which makes the slide almost completely reflective to mid-IR radiation while it still remains totally transparent to visible light. Therefore, the sample can be inspected by visible light in transmission, whereas mid-IR radiation passes through the sample, is reflected back by the coating on the low-e slide and then passing through the sample again directs to the detector. The resulting mid-IR spectrum is closely equivalent to a mid-IR transmission spectrum recorded from a sample of double the section thickness. This convenient method to obtain representative spectra of individual cells can be strongly affected by severe distortions associated with resonant Mie scattering. Therefore, spectra necessitate to be always corrected for Mie scattering before applying algorithms for the classification of spectra [108]. Principal advantages of transflection microFT-IR are that low-e microscope slides are inert and therefore suitable for cell culture, resist to high temperatures and therefore can be sterilized and reused, and are less costly than other biocompatible substrates such as CaF_2 and BaF_2.

Attenuated Total Reflectance (ATR) (**Figure 4**) is an internal reflection technique where the IR beam is directed through an internal reflection element (IRE) with higher refractive index, n_1, to the sample with a lower refractive index, n_2. The IRE element has the shape of a prism (or other geometric shape) and the crystal (ATR crystal) mounted in ATR objectives can be ZnSe or type IIa diamond (n_1 = 2.4), or Si (n_1 = 3.42), or Ge (n_1 = 4). This spectroscopic technique does not require a thin sample section is prepared and generates the mid-IR spectrum of the surface of probing sample placed into intimate contact

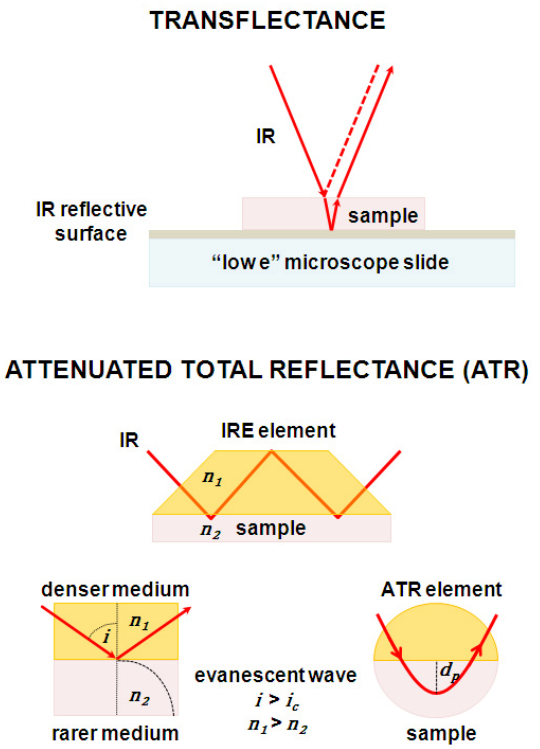

Figure 4. Transflectance and Attenuated Total Reflectance (ATR) techniques.

with the IRE element of ATR objective and can be utilize also in experiments with wet samples such as living cells [83]. Mid-IR radiation passing through the IRE will be totally internally reflected at the boundary separating the two media with $n_1 > n_2$ as well as it will provide an evanescent wave (decaying wave) that penetrates the surface of the sample with n_2 at an incident angle, i, that is greater than the critical angle, i_c. As a consequence, this evanescent wave will be attenuated by the mid-IR absorption characteristic of the lower refractive index medium and will provide IR data about sample composition [109]. The depth of penetration, d_p, of evanescent wave has direct dependence on wavelength, λ, so that the depth of surface layer probed increases with increasing λ. A procedure called ATR correction [64] allows generating a spectrum in which the relative intensity of bands can be corrected allowing the ATR spectrum becomes very similar to an IR spectrum recorded in transmission.

As for near-IR also mid-IR light can be coupled out of the spectrometer using silver halide (AgClBr) fiber optics that work as ATR elements [110]. Evanescent Wave Spectroscopy (EWS) is a new biophotonic technique based on the use of fiber optics in combination with IR spectroscopy. This very promising spectroscopic technique has many potential applications in preclinical and clinical cancer research and seems to realize the possibility to move IR spectroscopy and microscopy "from the bench to the bedside" [40, 111].

Analyses in the spectra

There are several different methods to approach the analysis of mid-IR spectra: from the simple inspection to identify the number of peaks to "chemometrics" where mathematical, statistical, and computer sciences methods are applied to improve the understanding of chemical information contained in typically broad and complex IR spectroscopic data [112]. Patterns in the data can be identified, modeled and must undergo independent validation [113] to be applied in probabilistic neural networks [114] useful for pre-clinical and clinical trials. It is the availability of validated models obtained by interdisciplinary approaches that may represent the actual limitation for the application of microFT-IR spectroscopy in pre-clinical and clinical trials on cancer.

Pre-processing (data set pre-processing) is required in order to reduce and correct interferences that may generate irrelevant variances such as atmospheric water vapour and carbon dioxide, variable background absorption profiles, and differences in sample thickness. Background intensity changes along the interval of wavenumebers that may alter the baseline are usually compensated by appropriate software methods for baseline correction (e.g.: Rubberband correction). However, baseline effects are almost completely removed and spectra with a mostly flat baseline are obtained also when the second derivative of an absorbance spectrum is calculated allowing, for instance to directly compare the spectra of individual eukaryotic cells. A number of specific software procedures are available to reduce variances related to the different pathlength in samples and normalize data sets. The choice of normalization is in general as crucial as the choice of the analysis technique itself. Rescaling the data, normalization makes different variables and different

Table 1. A summary of the vibrational frequencies of some functional groups in molecules within the mid -IR region of electromagnetic spectrum

Wavenumber (cm^{-1})	Functional group	Vibrational mode	Commonly assigned biochemical component
3500 - 2500	X-H stretching vibrations (where X is C, O, or N)		
~3300	N–H	ν(N–H)	Amide A: peptide, protein
~3100	N–H	ν(N–H)	Amide B: peptide, protein
2957	$C–CH_3$	$\nu_{as}(CH_3)$	lipids
2920	$–(CH_2)_n–$	$\nu_{as}(CH_2)$	
2872	$C–CH_3$	$\nu_s(CH_3)$	
2851	$–(CH_2)_n–$	$\nu_s(CH_2)$	
2000 - 1500	fundamental stretching vibrations of double bonds (e.g., C=O, C=C, C=N)		
~1740	$–CH_2–COOR$	ν(C=O)	Phospholipid esters
~1655	O=C–N–H	80% ν(CO), 20% ν(CN)	Amide I peptide, protein
~1645	H–O–H	γ(HOH)	Water
~1545	O=C–N–H	60% γ(N–H), 30% ν(C–N), 10% ν(C–C)	Amide II peptide, protein
~1500 - 600	the “fingerprinting region”: many overlapped vibrations		
~1450	$–(CH_3)_n–$ $–(CH_2)_n$	$\delta_{as}(CH_3)$ $\delta_{as}(CH_3)$	Lipid, protein
~1395	$–(CH_3)_n–$ $–(CH_2)_n$ $^-O–C=O$	$\delta_s(CH_3)$ $\delta_s(CH_3)$ ν(C=O)	Lipid, protein
~1380	$C–CH_3$	$\gamma_s(CH_3)$	Phospholipid, fatty acid, triglyceride
1400 - 1200	O=C–N–H, CH_3	γ(N–H), ν(C–N), γ(C=O), ν(C–C) and $\nu(CH_3)$	Amide III peptide, protein, collagen
~1245 - 1230	$RO–PO_2^-–OR$	$\nu_{as}(PO_2^-)$	DNA, RNA, phospholipid, phosphorylated protein
~1170	R–COO–R’	$\nu_{as}(C–O)$	Ester
~1160 and ~1120		ν(C–O)	RNA ribose
~1150	C–O, C–O–H	ν(CO), γ(COH)	carbohydrates
~1095, ~1084, ~1070	$RO–PO_2^-–OR$	$\nu_s(PO_2^-)$	DNA, RNA, phospholipid, phosphorylated protein
~1078	C–C	ν(CC)	glycogen
~1060, 1050, 1015	C–O	ν(CO)	DNA and RNA ribose
~1050	C–O–P	ν(COP)	Phosphate ester
~1028	C–O–H	def(CHO)	glycogen
~965	PO_3^{2-}	$\nu(PO_3^{2-})$	DNA and RNA ribose
~950	P–O	$\nu(PO_3^{2-})$	Phosphorylated protein
~920	C–O–P	ν(COP)	Phosphorylated protein

ν, stretching; δ, bending; γ, wagging, twisting, and rocking; def, deformation, as, antisymmetric; s, symmetric.

samples comparable allowing integrating them in a joint analysis.

The simple inspection of the mid-IR spectrum of a cell, for instance that of a human monocyte shown in **Figure 3a**, identifies the presence of some peaks. The identification and assignment of spectral components (marker peaks) is generally performed by the so-called “group frequency approach”. This represents a traditional

and still very popular method of spectral analysis. Frequency of vibration of specific functional groups is pre-assigned according to those observed in the mid-IR spectrum of corresponding pure biomolecules [115] or of mixtures of molecules [116] and compared with those already reported in the literature [117] and summarized in **Table 1**. However, much of the available information is purely explorative and has limited utility if not accompanied by an independent validation which appears of crucial importance to extend the number of potential applications of microFT-IR spectroscopy in cancer research and clinical diagnosis.

The characteristic features of a mid-IR absorbance spectrum of a cell are shown in **Figure 3a**. Major marker peaks are the Amide I and Amide II characterizing the spectrum of proteins and polypeptides. Amide I band absorbing at ~1650 cm^{-1} identifies the C=O stretching mode, νC=O, associated with vibrations of a secondary amide, –C(=O)N(H)–, whereas Amide II band absorbing at ~1550 cm^{-1} refers to the combination of both N–H bending and C–N stretching vibrations. Not only Amide I and Amide II identify protein molecule but their positions and shapes may reflect changes in the secondary protein structure [66]. Moreover, $\nu_{as}CH_3$ and $\nu_{as}CH_2$ observed at ~2958 cm^{-1} and at ~2920 cm^{-1} together with the ν_sCH_3 and ν_sCH_2 occurring at ~2872 cm^{-1} and at ~2852 cm^{-1}, respectively identify lipid molecules. The ν_{as} and $\nu_sPO_2^-$ stretching vibrations occurring at ~1240 cm^{-1} and at ~1085 cm^{-1} respectively can suggest the absorption of O–P=O linkages of the polynucleotide chains in DNA and RNA. The identification and assignment of major spectral components by "functional group analysis" is particularly useful for the qualitative analysis of pure organic molecules since the IR spectrum of each molecule is unique and it can serve as a signature to distinguish among different molecules, for instance pure proteins, nucleic acids DNA and RNA, lipids, and sugars. However, it is evident from **Table 1** that the IR spectrum of a cell usually contains a large number or bands, many of which will be impossible to confidently assign to vibration of a particular group, in particular analyzing the so called "fingerprinting region". Moreover, cell composes of many mid-IR active molecular constituents such as membrane lipids and phospholipids, glycolipids, proteins, glycoproteins, phosphoproteins, nucleic acids DNA and RNA, carbohydrates and a variety of small metabolites that may concur to spectral features. Therefore, we must conclude that the unequivocal interpretation of pre-assigned vibrational frequencies is impossible because the vibrations of different molecular components of a cell may overlap and the spectrum may reflect only the average biochemical composition.

The fact that more than one vibrational mode may concur in peaks requires the application of some type of "resolution enhancement" such as derivative spectroscopy (e.g. second-derivative) together with some de-noising filter (e.g.: smoothing) [64]. The analysis of derivative spectra is generally applied to identify the number of sub-band components that contribute within the peaks (**Figure 3a**). Generally sub-bands components below the spectral resolution are not considered. Fourier self-deconvolution (FSD) is another procedure that can be applied in an attempt to separate overlapping bands into single sub-bands that are broader than spectral resolution [118, 119]. However, the importance to obtain the highest S/N values becomes well evident comparing the second derivative spectra of **Figure 3a**. Both spectra have acceptable S/N values but there is much more uncertainty in the identification and assignment of subcomponents in the second derivative spectrum obtained with Globar than in the spectrum obtained with SR IR microFT-IR. Therefore the application of algorithms for self-deconvolution could erroneously identify a high number of subcomponents.

The calculation of difference spectrum is another way to obtain information on biochemical, functional, structural and dynamical changes occurring also in complex samples and in some circumstances to identify spectral components that may assume the significance of IR biomarkers [90]. For instance, during a typical time -course or dose-response experiment with cells, the vibrations from groups that do not change during the stimulation annihilated each other, and only the changes occurring as a consequence of the activation/inhibition become evident in the difference spectrum.

Two-dimensional IR correlation spectroscopy [120] is a perturbation-based method that monitors the perturbation-induced changes caused by the application of a stimulus at each wavenumber by microFT-IR. When an external perturbation (e.g.: an agonist or an inhibitor) is applied, the overall response of the stimulated system (e.g.: cell culture) to the applied pertur-

bation leads to distinctive intensity changes, band shifts, and changes in band shapes in the measured spectrum. A data set of so-called dynamic spectra are generated (e.g. within time but also concentration, temperature, etc. can be considered) and compositional changes can be probed, for instance over the course of time, t, on time scales ranging from a few milliseconds to hours, depending on the specific microFT-IR setup. By a correlation method the set of IR spectra are correlated (synchronous, asynchronous or other types of correlations) and a 2D cross-correlated spectrum is generated. In the 2D correlation spectrum the intensity of spectral changes at each frequency are plotted as a function of two independent frequency axes (Z and X) over the third dimension time, allowing the complex spectra can be visualized in the simplified form of fishnet and/or contour map. By this method of representing IR data many overlapped peaks are better resolved.

The different components identified within a spectrum can be quantified and compared among samples by univariate statistics. Since this limits to analyze individual components separately, it is not properly suitable for comparisons among large data set. Therefore the time-consuming univariate analysis is scarcely reliable for screening purposes. On the contrary, computer-based spectral analysis provides an objective method of scoring spectral information independently of subjective manual interpretation and therefore it may be potentially more sensitive, more consistent, and more accurate [121]. To analyze data sets of complex biological matrices such as cells and tissues powerful algorithms of multivariate statistical analysis can be applied [122].

Multivariate pattern recognition methods compare a large number of variables (e.g. absolute and relative intensity, the position, and the width of one or more absorptions) within a data set. In particular, multivariate classification with supervised or unsupervised pattern recognition can be applied. In supervised pattern recognition a substantial amount of information (e.g. biochemical or clinical data), is available regarding the data set (e.g.. which sample belongs to drug treated class or untreated control class, which cellular phenotype has been considered within a cancer cell line, etc.). In unsupervised pattern recognition no “a priori” knowledge about the data set is required (e.g.: the class membership) and the computer system groups or clusters the data by using a set of general rules [123]. The most popular techniques are Principal Component Analysis (PCA) and Cluster Analysis (CA). PCA is a non-parametric method for extracting relevant information from confusing data sets allowing to identify patterns in data and to highlight their similarities and differences [121]. PCA reduces the dimensionality, the number of variables of the data, by maintaining as much variance as possible [124]. Major benefit of PCA is that the large number of initial variables are condensed to only a few variables (the so called principal component), those reflecting the most relevant analytical information [125]. Hierarchical Cluster Analysis (HCA) follows a bottom-up strategy to discover unexpected clusters that may not be initially evident. It begins with each element (whole spectrum or selected intervals of frequencies) as a separate cluster and then finds clusters in a series of partitions on the basis of successively established clusters. An example of the unsupervised recognition of pattern is illustrated in **Figure 5**. Initially, the mid-IR spectra are pre-processed, for instance with vector normalization and second derivative. Then Euclidean distances among the comparable spectra are calculated by a standard method. Euclidean distance is a descriptor of the degree of similarity among two spectra or two clusters: the better two spectra (or clusters) match, the smaller the spectral distance. Finally, an algorithm usually performs the clustering process. For instance, Ward’s algorithm has been applied to obtain cluster distances shown in the dendrogram of **Figure 5a**. Instead of determining the spectral distance, this algorithm tries to find as homogeneous groups as possible merging only the two groups with the smallest growth in heterogeneity factor, H. At the end, only two groups are remained, for instance viable (G0-G1 phase) and apoptotic cells whose average spectra are shown in **Figure 5b**, respectively. This technique does not require assumption to be made about the number of data groups and has assumed great popularity, for instance to classify bacteria [58] and eukaryotic cells [57], mostly due to its simplicity and ease of interpretation.

Other than in histopathology other application of microFT-IR might include evaluation of drug efficacy in both cellular models used for drug screening or primary cells obtained from individual patients. In line with these possibilities we

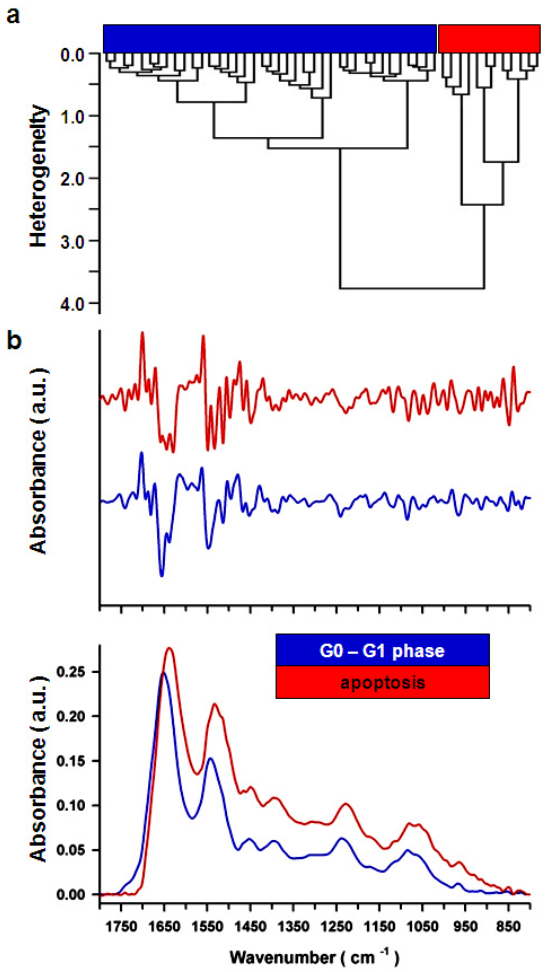

Figure 5. The unsupervised recognition of spontaneous apoptosis in the spectra of MEG-01 leukemic blasts. **a**. Hierarchical Cluster Analysis (HCA), was applied to several spectra of individual MEG-01 blasts that had been obtained by SR microFT-IR absorbance spectroscopy performed at the beamline B22 Infrared Microspectroscopy end station of Diamond Light Source (probing area: 15 μm x 15 μm either in the sample and in the background; IR source: Synchrotron Radiation; detector: MCT with a 50 μm^2 detecting area; IR sampling interval: 4000-700 cm^{-1}, number of scans: 128; scanner velocity 40 kHz; spectral sensitivity 4 cm^{-1}). HCA was performed by a standard method and Ward's algorithm applied to the interval of frequencies 1780-1480 cm^{-1} in the spectra pre-treated with vector normalization and second derivative calculated with the Savitzky-Golay smoothing algorithm on 9 points. **b**. The two spectral patterns representative of apoptotic (red trace) and G0-G1 viable (blue trace) MEG-01 cells were obtained by averaging parental spectra clustered by HCA in each of the two final groups, respectively. Typical IR signatures of cell apoptosis are the shift of amide I and amide II peaks towards lower wavenumbers and the increased absorbance at ~1740 cm^{-1} assigned to the C=O in phospholipid. Independent validation of IR data was obtained by the analysis of apoptotic events carried out in parallel samples by complementary techniques (data not shown).

could associate a specific region of mid-IR absorbance spectrum to the reduction in tyrosine phosphorylation in K562 cells following treatment with the tyrosine kinase inhibitor (TKI) imatinib-mesylate, the founder of a class of highly effective BCR/ABL inhibitors of clinical efficacy [126]. This procedure identified a useful biomarker of drug efficacy and has been cross-validated with conventional methods [98]. De facto TKIs represent the current state-of-the-art for the cure of CML [127] and the possibility to monitor ex vivo, with minimal sample treatment, the efficacy of TKI treatment in the individual patient by microFT-IR can represent a step forward for a more efficient and targeted personalized medicine.

4. Towards the use of mid-IR spectrum as a marker of cancer and anticancer therapy follow up

Generally we refer to a cancer biomarker as a specific gene or a more or less expressed protein or protein activity or as some "…omics" profiles. Therefore we approach mid-IR analyses in search of some specific vibrational components with the equivalent significance of a traditional cancer biomarker. On the contrary, what the mid-IR spectrum of a cell reflects is the overall vibrations of cell components and their interaction within the sample. Therefore, specific protein components, for instance BCR/ABL oncoprotein, cannot be directly measured in the spectrum of K562 cells without some labeling and/or other forms of pre-treatment in samples and in the absence of a calibration method [75]. Due to the lack of such specific molecular information, many are skeptics about the possibility that the mid-IR absorbance spectrum, which snapshots the whole biochemical compo-

sition of a cell and that is sensitive to structural changes, can be used as a biomarker of cancer or of cancer progression or of anticancer therapy efficacy. With the attempt to move microFT-IR "from bench top to bedside" new powerful algorithm for automatic data analysis and treatment of large data sets have been therefore developed allowing the easy interpretation of IR data also by non spectroscopists. Examples concerning with the reliability in applying microFT-IR for screening and early diagnosis of cancer are cervical cancer [31], exfoliative cytology [128], and the analysis of multiple prostate biopsies where different cell components within a tissue might be identified by qualitative and quantitative analysis allowing to be correctly classified by objective criteria [57].

5. Conclusions

The main limitations of microFT-IR spectroscopy can be summarized in its relatively low spatial resolution limited to the sizes of a cell and a certain difficulty to analyze wet samples. Other factors are commonly shared with many other methods. On the contrary advantages are represented by the possibility to obtain biochemical information on molecular composition and structure at the level of single cell within a timescale of few seconds-minutes and to perform qualitative and quantitative multi-component analyses allowing automated pattern recognition and objective classifications in samples with minimal and label-free sample treatment (mostly formalin fixation followed by wash in water and dehydration). The hope is not only that technical improvements will progressively increase the number of potential applications of microFT-IR to cancer research and clinical diagnosis but also that in the next future pre-clinical and clinical trials will include sample evaluation utilizing this technique in order to obtain data necessary to validate the use of microFT-IR spectroscopy in a clinical context. In fact, this appears to be the most important way to reduce the too high level of skepticism of many biologists and pathologists about an old technology that has been designed and improved mainly for applications in cancer research and clinical diagnosis.

6. Acknowledgements

The research leading to the results presented in this review has received funding from the European Community's Seventh Framework Programme (FP7/2007-2013) under grant agreement no. 226716. We thank Diamond Light Source (DLS) for access to the beamline B22 Infrared Microspectroscopy (proposals sm 4333 and sm 6675). The support of beamline staff was essential and in particular we acknowledge the principal beamline scientist Dr. Gianfelice Cinque.We also acknowledge the contribution of AIRC (IG4667) to CS and Dr. Marzia Vezzalini who cultivated cells used in experiments at DLS.

Address correspondence to: Giuseppe Bellisola, Department of Pathology and Diagnostics, Unit of Immunology, Azienda Ospedaliera Universitaria Integrata Verona, Verona, Italy Tel: +39 045 8126451; Fax: +39 045 8126455; E-mail: giuseppe.bellisola@univr.it or to Claudio Sorio, Department of Pathology and Diagnostics, General Pathology Section, University of Verona, Verona, Italy Tel: +39-045-8027688; Fax: +39-045-8027127; E-mail: claudio.sorio@univr.it

References

[1] Stratton MR. Exploring the genomes of cancer cells: progress and promise. Science 2011; 331: 1553-1558.

[2] Tsai HC, Baylin SB. Cancer epigenetics: linking basic biology to clinical medicine. Cell Res 2011; 21: 502-517.

[3] Loeb LA. Human cancers express mutator phenotypes: origin, consequences and targeting. Nat Rev Cancer 2011; 11: 450-457.

[4] Payne SJ, Jones L. Influence of the tumor microenvironment on angiogenesis. Future Oncol 2011; 7: 395-408.

[5] Quezada SA, Peggs KS, Simpson TR and Allison JP. Shifting the equilibrium in cancer immunoediting: from tumor tolerance to eradication. Immunol Rev 2011; 241: 104-118.

[6] Solyanik GI. Multifactorial nature of tumor drug resistance. Exp Oncol 2010; 32: 181-185.

[7] Jemal A, Bray F, Center MM, Ferlay J, Ward E and Forman D. Global cancer statistics. CA Cancer J Clin 2011; 61: 69-90.

[8] Coyle YM. Lifestyle, genes, and cancer. Methods Mol Biol 2009; 472: 25-56.

[9] Jha P. Avoidable global cancer deaths and total deaths from smoking. Nat Rev Cancer 2009; 9: 655-664.

[10] Hanash SM, Baik CS and Kallioniemi O. Emerging molecular biomarkers-blood-based strategies to detect and monitor cancer. Nat Rev Clin Oncol 2011; 8: 142-150.

[11] Arthur J Atkinson Jr, Wayne A Colburn, Victor G DeGruttola, David L DeMets, Gregory J DowningDO, Daniel F Hoth, John A Oates, Carl C Peck, Robert T Schooley, Bert A Spilker,

Janet Woodcock and Scott L Zeger. Biomarkers and surrogate endpoints: preferred definitions and conceptual framework. Clin Pharmacol Ther 2001; 69: 89-95.
[12] Ioannidis JP, Castaldi P and Evangelou E. A compendium of genome-wide associations for cancer: critical synopsis and reappraisal. J Natl Cancer Inst 2010; 102: 846-858.
[13] Turtoi A, De Pauw E and Castronovo V. Innovative proteomics for the discovery of systemically accessible cancer biomarkers suitable for imaging and targeted therapies. Am J Pathol 2011; 178: 12-18.
[14] Chandra H, Reddy PJ and Srivastava S. Protein microarrays and novel detection platforms. Expert Rev Proteomics 2011; 8: 61-79.
[15] Sharma SV, Haber DA and Settleman J. Cell line-based platforms to evaluate the therapeutic efficacy of candidate anticancer agents. Nat Rev Cancer 2010; 10: 241-253.
[16] Milestones in light microscopy. Nat Cell Biol 2009; 11: 1165.
[17] Fortney K, Jurisica I. Integrative computational biology for cancer research. Hum Genet 2011; 130: 465-481.
[18] Blake PM, Decker DA, Glennon TM, Liang YM, Losko S, Navin N and Suh KS. Toward an integrated knowledge environment to support modern oncology. Cancer J 2011; 17: 257-263.
[19] Dunn BK, Jegalian K and Greenwald P. Biomarkers for early detection and as surrogate endpoints in cancer prevention trials: issues and opportunities. Recent Results Cancer Res 2011; 188: 21-47.
[20] Van't Westeinde SC, van Klaveren RJ. Screening and early detection of lung cancer. Cancer J 2011; 17: 3-10.
[21] Hell SW. Far-field optical nanoscopy. Science 2007; 316: 1153-1158.
[22] Pysz MA, Gambhir SS and Willmann JK. Molecular imaging: current status and emerging strategies. Clin Radiol 2010; 65: 500-516.
[23] Condeelis J, Weissleder R. In vivo imaging in cancer. Cold Spring Harb Perspect Biol 2010; 2: a003848.
[24] Naumov GN, Bender E, Zurakowski D, Kang SY, Sampson D, Flynn E, Watnick RS, Straume O, Akslen LA, Folkman J and Almog N. A model of human tumor dormancy: an angiogenic switch from the nonangiogenic phenotype. J Natl Cancer Inst 2006; 98: 316-325.
[25] Seigneuric R, Markey L, Nuyten DS, Dubernet C, Evelo CT, Finot E and Garrido C. From nanotechnology to nanomedicine: applications to cancer research. Curr Mol Med 2010; 10: 640-652.
[26] Perini R, Choe R, Yodh AG, Sehgal C, Divgi CR and Rosen MA. Non-invasive assessment of tumor neovasculature: techniques and clinical applications. Cancer Metastasis Rev 2008; 27: 615-630.
[27] Barer R, Cole AR and Thompson HW. Infra-red spectroscopy with the reflecting microscope in physics, chemistry and biology. Nature 1949; 163: 198-201.
[28] Blout ER, Mellors RC. Infrared Spectra of Tissues. Science 1949; 110: 137-138.
[29] Woernley DL. Infrared absorption curves for normal and neoplastic tissues and related biological substances. Cancer Res 1952; 12: 516-523.
[30] Fisher SE, Harris AT, Khanna N and Sule-Suso J. Vibrational spectroscopy: what does the clinician need? In David Moss ed.: Biomedical applications of synchrotron infrared microspectroscopy. A practical approach. Cambridge, UK: RSC Publishing, 2011.
[31] Matthaus C, Bird B, Miljkovic M, Chernenko T, Romeo M and Diem M. Chapter 10: Infrared and Raman microscopy in cell biology. Methods Cell Biol 2008; 89: 275-308.
[32] Mostaco Guidolin LB, Bachmann L. Application of FTIR Spectroscopy for Identification of Blood and Leukemia Biomarkers: A Review over the Past 15 Years. Applied Spectroscopy Reviews 2011; 46: 388-404.
[33] Liu KZ, Xu M and Scott DA. Biomolecular characterisation of leucocytes by infrared spectroscopy. Br J Haematol 2007; 136: 713-722.
[34] Petter CH, Heigl N, Rainer M, Bakry R, Pallua J, Bonn GK and Huck CW. Development and application of Fourier-transform infrared chemical imaging of tumour in human tissue. Curr Med Chem 2009; 16: 318-326.
[35] Walsh MJ, German MJ, Singh M, Pollock HM, Hammiche A, Kyrgiou M, Stringfellow HF, Paraskevaidis E, Martin-Hirsch PL and Martin FL. IR microspectroscopy: potential applications in cervical cancer screening. Cancer Lett 2007; 246: 1-11.
[36] Rehman IU, Rehman S, Movasaghi Z and Darr JA. Fourier Transform Infrared Spectroscopic Analysis of Breast Cancer Tissues; Identifying Differences between Normal Breast, Invasive Ductal Carcinoma, and Ductal Carcinoma In Situ of the Breast. Applied Spectroscopy Reviews 2010; 45: 355-368.
[37] Jackson M, Mansfield JR, Dolenko B, Somorjai RL, Mantsch HH and Watson PH. Classification of breast tumors by grade and steroid receptor status using pattern recognition analysis of infrared spectra. Cancer Detect Prev 1999; 23: 245-253.
[38] Kwak JT, Hewitt SM, Sinha S and Bhargava R. Multimodal microscopy for automated histologic analysis of prostate cancer. BMC Cancer 2011; 11: 62.
[39] Lewis PD, Lewis KE, Ghosal R, Bayliss S, Lloyd AJ, Wills J, Godfrey R, Kloer P and Mur LA. Evaluation of FTIR spectroscopy as a diagnostic tool for lung cancer using sputum. BMC Cancer 2010; 10: 640.
[40] Sahu RK, Mordechai S. Spectral signatures of

colonic malignancies in the mid-infrared region: from basic research to clinical applicability. Future Oncol 2010; 6: 1653-1667.
[41] Travo A, Piot O, Wolthuis R, Gobinet C, Manfait M, Bara J, Forgue Lafitte ME and Jeannesson P. IR spectral imaging of secreted mucus: a promising new tool for the histopathological recognition of human colonic adenocarcinomas. Histopathology 2010; 56: 921-931.
[42] Wehbe K, Pineau R, Eimer S, Vital A, Loiseau H and Deleris G. Differentiation between normal and tumor vasculature of animal and human glioma by FTIR imaging. Analyst 2010; 135: 3052-3059.
[43] Krafft C, Sobottka SB, Geiger KD, Schackert G and Salzer R. Classification of malignant gliomas by infrared spectroscopic imaging and linear discriminant analysis. Anal Bioanal Chem 2007; 387: 1669-1677.
[44] Petibois C, Deleris G. Chemical mapping of tumor progression by FT-IR imaging: towards molecular histopathology. Trends Biotechnol 2006; 24: 455-462.
[45] Wong PT, Goldstein SM, Grekin RC, Godwin TA, Pivik C and Rigas B. Distinct infrared spectroscopic patterns of human basal cell carcinoma of the skin. Cancer Res 1993; 53: 762-765.
[46] Hammody Z, Argov S, Sahu RK, Cagnano E, Moreh R and Mordechai S. Distinction of malignant melanoma and epidermis using IR micro-spectroscopy and statistical methods. Analyst 2008; 133: 372-378.
[47] Eikje NS, Aizawa K, Sota T, Ozaki Y and Arase S. Identification and characterization of skin biomolecules for drug targeting and monitoring by vibrational spectroscopy. Open Med Chem J 2008; 2: 38-48.
[48] Quaroni L, Casson AG. Characterization of Barrett esophagus and esophageal adenocarcinoma by Fourier-transform infrared microscopy. Analyst 2009; 134: 1240-1246.
[49] Le Naour F, Bralet MP, Debois D, Sandt C, Guettier C, Dumas P, Brunelle A and Laprevote O. Chemical imaging on liver steatosis using synchrotron infrared and ToF-SIMS microspectroscopies. PLoS One 2009; 4: e7408.
[50] Bird B, Miljkovic M, Romeo MJ, Smith J, Stone N, George MW and Diem M. Infrared microspectral imaging: distinction of tissue types in axillary lymph node histology. BMC Clin Pathol 2008; 8: 8.
[51] Liu KZ, Jia L, Kelsey SM, Newland AC and Mantsch HH. Quantitative determination of apoptosis on leukemia cells by infrared spectroscopy. Apoptosis 2001; 6: 269-278.
[52] Kelly JG, Nakamura T, Kinoshita S, Fullwood NJ and Martin FL. Evidence for a stem-cell lineage in corneal squamous cell carcinoma using synchrotron-based Fourier-transform infrared microspectroscopy and multivariate analysis. Analyst 2010; 135: 3120-3125.
[53] Walsh MJ, Hammiche A, Fellous TG, Nicholson JM, Cotte M, Susini J, Fullwood NJ, Martin-Hirsch PL, Alison MR and Martin FL. Tracking the cell hierarchy in the human intestine using biochemical signatures derived by mid-infrared microspectroscopy. Stem Cell Res 2009; 3: 15-27.
[54] Ami D, Neri T, Natalello A, Mereghetti P, Doglia SM, Zanoni M, Zuccotti M, Garagna S and Redi CA. Embryonic stem cell differentiation studied by FT-IR spectroscopy. Biochim Biophys Acta 2008; 1783: 98-106.
[55] Krafft C, Salzer R, Seitz S, Ern C and Schieker M. Differentiation of individual human mesenchymal stem cells probed by FTIR microscopic imaging. Analyst 2007; 132: 647-653.
[56] Grude O, Hammiche A, Pollock H, Bentley AJ, Walsh MJ, Martin FL and Fullwood NJ. Near-field photothermal microspectroscopy for adult stem-cell identification and characterization. J Microsc 2007; 228: 366-372.
[57] Bhargava R, Fernandez DC, Hewitt SM and Levin IW. High throughput assessment of cells and tissues: Bayesian classification of spectral metrics from infrared vibrational spectroscopic imaging data. Biochim Biophys Acta 2006; 1758: 830-845.
[58] Naumann D, Helm D and Labischinski H. Microbiological characterizations by FT-IR spectroscopy. Nature 1991; 351: 81-82.
[59] Preisner O, Lopes JA, Guiomar R, Machado J and Menezes JC. Fourier transform infrared (FT-IR) spectroscopy in bacteriology: towards a reference method for bacteria discrimination. Anal Bioanal Chem 2007; 387: 1739-1748.
[60] Nasse MJ, Walsh MJ, Mattson EC, Reininger R, Kajdacsy-Balla A, Macias V, Bhargava R and Hirschmugl CJ. High-resolution Fourier-transform infrared chemical imaging with multiple synchrotron beams. Nat Methods 2011; 8: 413-416.
[61] Petibois C, Desbat B. Clinical application of FTIR imaging: new reasons for hope. Trends Biotechnol 2010; 28: 495-500.
[62] Meier RJ. Vibrational spectroscopy: a 'vanishing' discipline? Chem Soc Rev 2005; 34: 743-752.
[63] Chalmers JM, Griffiths PR. Handbook of vibrational spectroscopy. New York: J. Wiley, 2002.
[64] Griffiths PR, De Haseth JA. Fourier transform infrared spectrometry. Hoboken, NJ: Wiley-Interscience, 2007.
[65] Diem M, Chalmers JM and Griffiths PR. Vibrational spectroscopy for medical diagnosis. Chichester, England ; Hoboken, NJ: John Wiley & Sons, 2008.
[66] Barth A. Infrared spectroscopy of proteins. Biochim Biophys Acta 2007; 1767: 1073-1101.
[67] Zhang Y, Hong H and Cai W. Imaging with Raman spectroscopy. Curr Pharm Biotechnol 2010; 11: 654-661.

[68] Swain RJ, Stevens MM. Raman microspectroscopy for non-invasive biochemical analysis of single cells. Biochem Soc Trans 2007; 35: 544-549.
[69] Barr H, Kendall C, Hutchings J, Bazant-Hegemark F, Shepherd N and Stone N. Rapid endoscopic identification and destruction of degenerating Barrett's mucosal neoplasia. Surgeon 2011; 9: 119-123.
[70] Lasch P, Naumann D. Spatial resolution in infrared microspectroscopic imaging of tissues. Biochim Biophys Acta 2006; 1758: 814-829.
[71] Carr GL. Resolution limits for infrared microspectroscopy explored with synchrotron radiation. Review of Scientific Instruments 2001; 72: 1613-1619.
[72] Dumas P, Sockalingum GD and Sule-Suso J. Adding synchrotron radiation to infrared microspectroscopy: what's new in biomedical applications? Trends Biotechnol 2007; 25: 40 -44.
[73] Miller LM and Dumas P. Chemical imaging of biological tissue with synchrotron infrared light. Biochim Biophys Acta 2006; 1758: 846-857.
[74] Levin IW, Bhargava R. Fourier transform infrared vibrational spectroscopic imaging: integrating microscopy and molecular recognition. Annu Rev Phys Chem 2005; 56: 429-474.
[75] Petibois C, Gionnet K, Goncalves M, Perromat A, Moenner M and Deleris G. Analytical performances of FT-IR spectrometry and imaging for concentration measurements within biological fluids, cells, and tissues. Analyst 2006; 131: 640-647.
[76] Garidel P, Boese M. Mid infrared microspectroscopic mapping and imaging: a bioanalytical tool for spatially and chemically resolved tissue characterization and evaluation of drug permeation within tissues. Microsc Res Tech 2007; 70: 336-349.
[77] Masuch R, Moss DA. Stopped flow apparatus for time-resolved Fourier transform infrared difference spectroscopy of biological macromolecules in 1H2O. Appl Spectrosc 2003; 57: 1407-1418.
[78] Bogomolny E, Argov S, Mordechai S and Huleihel M. Monitoring of viral cancer progression using FTIR microscopy: a comparative study of intact cells and tissues. Biochim Biophys Acta 2008; 1780: 1038-1046.
[79] Ostrowska KM, Garcia A, Meade AD, Malkin A, Okewumi I, O'Leary JJ, Martin C, Byrne HJ and Lyng FM. Correlation of p16(INK4A) expression and HPV copy number with cellular FTIR spectroscopic signatures of cervical cancer cells. Analyst 2011; 136: 1365-1373.
[80] Steiner G, Shaw A, Choo Smith LP, Abuid MH, Schackert G, Sobottka S, Steller W, Salzer R and Mantsch HH. Distinguishing and grading human gliomas by IR spectroscopy. Biopolymers 2003; 72: 464-471.
[81] Gasper R, Dewelle J, Kiss R, Mijatovic T and Goormaghtigh E. IR spectroscopy as a new tool for evidencing antitumor drug signatures. Biochim Biophys Acta 2009; 1788: 1263-1270.
[82] Krishna CM, Kegelaer G, Adt I, Rubin S, Kartha VB, Manfait M and Sockalingum GD. Combined Fourier transform infrared and Raman spectroscopic approach for identification of multidrug resistance phenotype in cancer cell lines. Biopolymers 2006; 82: 462-470.
[83] Holman HYN, Bechtel HA, Hao Z and Martin MC. Synchrotron IR Spectromicroscopy: Chemistry of Living Cells. Analytical Chemistry 2010; 82: 8757-8765.
[84] Gazi E, Dwyer J, Lockyer NP, Miyan J, Gardner P, Hart C, Brown M and Clarke NW. Fixation protocols for subcellular imaging by synchrotron-based Fourier transform infrared microspectroscopy. Biopolymers 2005; 77: 18-30.
[85] Jamin N, Dumas P, Moncuit J, Fridman WH, Teillaud JL, Carr GL and Williams GP. Highly resolved chemical imaging of living cells by using synchrotron infrared microspectrometry. Proc Natl Acad Sci USA 1998; 95: 4837-4840.
[86] Holman HY, Bjornstad KA, McNamara MP, Martin MC, McKinney WR and Blakely EA. Synchrotron infrared spectromicroscopy as a novel bioanalytical microprobe for individual living cells: cytotoxicity considerations. J Biomed Opt 2002; 7: 417-424.
[87] Moss DA, Keese M and Pepperkok R. IR micro spectroscopy of live cells. Vibrational Spectroscopy 2005; 38: 185-191.
[88] Birarda G, Grenci G, Businaro L, Marmiroli B, Pacor S and Vaccari L. Fabrication of a microfluidic platform for investigating dynamic biochemical processes in living samples by FTIR microspectroscopy. Microelectronic Engineering 2010; 87: 806-809.
[89] Davis BJ, Carney PS and Bhargava R. Theory of mid-infrared absorption microspectroscopy: II. Heterogeneous samples. Anal Chem 2010; 82: 3487-3499.
[90] Kotting C, Suveyzdis Y, Bojja RS, Metzler-Nolte N and Gerwert K. Label-free screening of drug-protein interactions by time-resolved Fourier transform infrared spectroscopic assays exemplified by Ras interactions. Appl Spectrosc 2010; 64: 967-972.
[91] Walsh MJ, Fellous TG, Hammiche A, Lin WR, Fullwood NJ, Grude O, Bahrami F, Nicholson JM, Cotte M, Susini J, Pollock HM, Brittan M, Martin-Hirsch PL, Alison MR and Martin FL. Fourier transform infrared microspectroscopy identifies symmetric PO(2)(-) modifications as a marker of the putative stem cell region of human intestinal crypts. Stem Cells 2008; 26: 108-118.
[92] Chonanant C, Jearanaikoon N, Leelayuwat C, Limpaiboon T, Tobin MJ, Jearanaikoon P and

Heraud P. Characterisation of chondrogenic differentiation of human mesenchymal stem cells using synchrotron FTIR microspectroscopy. Analyst 2011; 136: 2542-2551.
[93] Diem M, Boydston White S and Chiriboga L. Infrared spectroscopy of cells and tissues: Shining light onto a novel subject. Applied Spectroscopy 1999; 53: 148a-161a.
[94] Holman HY, Martin MC, Blakely EA, Bjornstad K and McKinney WR. IR spectroscopic characteristics of cell cycle and cell death probed by synchrotron radiation based Fourier transform IR spectromicroscopy. Biopolymers 2000; 57: 329-335.
[95] Pacifico A, Chiriboga LA, Lasch P and Diem M. Infrared spectroscopy of cultured cells - II. Spectra of exponentially growing, serum-deprived and confluent cells. Vibrational Spectroscopy 2003; 32: 107-115.
[96] Zelig U, Kapelushnik J, Moreh R, Mordechai S and Nathan I. Diagnosis of cell death by means of infrared spectroscopy. Biophys J 2009; 97: 2107-2114.
[97] Gault N, Lefaix JL. Infrared microspectroscopic characteristics of radiation-induced apoptosis in human lymphocytes. Radiat Res 2003; 160: 238-250.
[98] Bellisola G, Della Peruta M, Vezzalini M, Moratti E, Vaccari L, Birarda G, Piccinini M, Cinque G and Sorio C. Tracking infrared signatures of drugs in cancer cells by Fourier transform microspectroscopy. Analyst 2010; 135: 3077-3086.
[99] Di Giambattista L, Pozzi D, Grimaldi P, Gaudenzi S, Morrone S and Castellano AC. New marker of tumor cell death revealed by ATR-FTIR spectroscopy. Anal Bioanal Chem 2011; 399: 2771-2778.
[100] Le Gal JM, Morjani H and Manfait M. Ultrastructural appraisal of the multidrug resistance in K562 and LR73 cell lines from Fourier transform infrared spectroscopy. Cancer Res 1993; 53: 3681-3686.
[101] Manfait M, Theophanides T. Fourier transform infrared spectra of cells treated with the drug adriamycin. Biochem Biophys Res Commun 1983; 116: 321-326.
[102] Gasparri F, Muzio M. Monitoring of apoptosis of HL60 cells by Fourier-transform infrared spectroscopy. Biochem J 2003; 369: 239-248.
[103] Boydston White S, Gopen T, Houser S, Bargonetti J and Diem M. Infrared spectroscopy of human tissue. V. Infrared spectroscopic studies of myeloid leukemia (ML-1) cells at different phases of the cell cycle. Biospectroscopy 1999; 5: 219-227.
[104] Mohlenhoff B, Romeo M, Diem M and Wood BR. Mie-type scattering and non-Beer-Lambert absorption behavior of human cells in infrared microspectroscopy. Biophys J 2005; 88: 3635-3640.
[105] Bassan P, Byrne HJ, Bonnier F, Lee J, Dumas P and Gardner P. Resonant Mie scattering in infrared spectroscopy of biological materials-understanding the 'dispersion artefact'. Analyst 2009; 134: 1586-1593.
[106] Bassan P, Kohler A, Martens H, Lee J, Byrne HJ, Dumas P, Gazi E, Brown M, Clarke N and Gardner P. Resonant Mie scattering (RMieS) correction of infrared spectra from highly scattering biological samples. Analyst 2010; 135: 268-277.
[107] Lee J, Gazi E, Dwyer J, Brown MD, Clarke NW, Nicholson JM and Gardner P. Optical artefacts in transflection mode FTIR microspectroscopic images of single cells on a biological support: the effect of back-scattering into collection optics. Analyst 2007; 132: 750-755.
[108] Harvey TJ, Gazi E, Henderson A, Snook RD, Clarke NW, Brown M and Gardner P. Factors influencing the discrimination and classification of prostate cancer cell lines by FTIR microspectroscopy. Analyst 2009; 134: 1083-1091.
[109] Bogomolny E, Huleihel M, Salman A, Zwielly A, Moreh R and Mordechai S. Attenuated total reflectance spectroscopy: a promising technique for early detection of premalignancy. Analyst 2010; 135: 1934-1940.
[110] Raichlin Y, Fel L and Katzir A. Evanescent-wave infrared spectroscopy with flattened fibers as sensing elements. Opt Lett 2003; 28: 2297-2299.
[111] Mackanos MA, Contag CH. Fiber-optic probes enable cancer detection with FTIR spectroscopy. Trends Biotechnol 2010; 28: 317-323.
[112] Lavine B, Workman J. Chemometrics. Anal Chem 2010; 82: 4699-4711.
[113] Lasch P, Diem M, Hansch W and Naumann D. Artificial neural networks as supervised techniques for FT-IR microspectroscopic imaging. J Chemom 2007; 20: 209-220.
[114] Podshyvalov A, Sahu RK, Mark S, Kantarovich K, Guterman H, Goldstein J, Jagannathan R, Argov S and Mordechai S. Distinction of cervical cancer biopsies by use of infrared microspectroscopy and probabilistic neural networks. Appl Opt 2005; 44: 3725-3734.
[115] Pevsner A, Diem M. IR spectroscopic studies of major cellular components. III. Hydration of protein, nucleic acid, and phospholipid films. Biopolymers 2003; 72: 282-289.
[116] Benedetti E, Benedetti E, Bramanti E, Papineschi F and Rossi I. Determination of the relative amount of nucleic acids and proteins in leukemic and normal lymphocytes by means of Fourier transform infrared microspectroscopy. Applied Spectroscopy 1997; 51: 792-797.
[117] Rehman IU, Movasaghi Z and Rehman S. Fourier transform infrared (FTIR) spectroscopy of biological tissues. Applied Spectroscopy Reviews 2008; 43: 134-179.

[118] Kauppinen JK, Moffatt DJ, Cameron DG and Mantsch HH. Noise in Fourier self-deconvolution. Appl Opt 1981; 20: 1866-1879.
[119] Mcclure WF, Davies AMC. Fourier Self-Deconvolution in the Analysis of near-Infrared Spectra of Chemically Complex Samples. Mikrochimica Acta 1988; 1: 93-96.
[120] Noda I, Ozaki Y. Two-dimensional correlation spectroscopy: applications in vibrational and optical spectroscopy. Chichester: J Wiley, 2004.
[121] Krafft C, Steiner G, Beleites C and Salzer R. Disease recognition by infrared and Raman spectroscopy. J Biophotonics 2009; 2: 13-28.
[122] Wang L, Mizaikoff B. Application of multivariate data-analysis techniques to biomedical diagnostics based on mid-infrared spectroscopy. Anal Bioanal Chem 2008; 391: 1641-1654.
[123] Frades I, Matthiesen R. Overview on techniques in cluster analysis. Methods Mol Biol 2010; 593: 81-107.
[124] Jolliffe IT. Principal component analysis. New York: Springer, 2002.
[125] Li L. Dimension reduction for high-dimensional data. Methods Mol Biol 2010; 620: 417-434.
[126] Deininger MW, Druker BJ. Specific targeted therapy of chronic myelogenous leukemia with imatinib. Pharmacol Rev 2003; 55: 401-423.
[127] Fullmer A, Kantarjian H, Cortes J and Jabbour E. New developments in the treatment of chronic myeloid leukemia and Philadelphia-positive acute lymphoblastic leukemia. Leuk Lymphoma 2011; 52 Suppl 1: 81-91.
[128] Bird B, Romeo MJ, Diem M, Bedrossian K, Laver N and Naber S. Cytology by Infrared Micro-Spectroscopy: Automatic Distinction of Cell Types in Urinary Cytology. Vib Spectrosc 2008; 48: 101-106.